J Appl Electrochem (2013) 43:271–278
DOI 10.1007/s10800-012-0517-y

ORIGINAL PAPER

Impact of microwave synthesis conditions on the rechargeable capacity of $LiCoPO_4$ for lithium ion batteries

Reginald E. Rogers · Garry M. Clarke · Olivia N. Matthew · Matthew J. Ganter · Roberta A. DiLeo · Jason W. Staub · Michael W. Forney · Brian J. Landi

Received: 29 August 2012 / Accepted: 11 December 2012 / Published online: 21 December 2012

Abstract Lithium transition metal phosphates have the capability of improving cathode energy densities up to 800 Wh kg^{-1}, a 27 % increase over conventional cathode active material energy densities. In this study, the effect of base-to-acid (NH_4OH:H_3PO_4) stoichiometric conditions on the intrinsic reversible capacity of lithium cobalt phosphate ($LiCoPO_4$) active material are investigated through microwave synthesis and electrochemical testing. Variation in solution pH results in an increase of 69 mAh g^{-1} in achievable capacity. X-ray diffraction results show highly crystalline $LiCoPO_4$, with particle sizes ranging from 200 nm to greater than 1 μm based upon scanning electron microscopy. Electrochemical analysis with 1 M $LiPF_6$ EC:EMC (1:2 v/v) provides the highest capacity over multiple cycles. A discharge capacity of 128 mAh g^{-1} (78 % of theoretical capacity) is achievable for intrinsic $LiCoPO_4$ without further treatment (e.g., carbon coating) at an effective 0.1 C rate with a proper constant current–constant voltage step. Analysis of reported synthesis techniques shows that microwave synthesis yields the highest capacity for the intrinsic $LiCoPO_4$ material to date.

Keywords Batteries · Lithium cobalt phosphate · Microwave synthesis · Nanomaterials

R. E. Rogers · G. M. Clarke · O. N. Matthew · B. J. Landi (✉)
Department of Chemical and Biomedical Engineering, Rochester Institute of Technology, Rochester, NY 14623, USA
e-mail: brian.landi@rit.edu

R. E. Rogers · M. J. Ganter · R. A. DiLeo · J. W. Staub · M. W. Forney · B. J. Landi
NanoPower Research Laboratories, Rochester Institute of Technology, Rochester, NY 14623, USA

M. J. Ganter
Golisano Institute for Sustainability, Rochester Institute of Technology, Rochester, NY 14623, USA

R. A. DiLeo
Microsystems Engineering, Rochester Institute of Technology, Rochester, NY 14623, USA

1 Introduction

Lithium ion battery technology is at the forefront of development to meet the growing electrical storage needs presented by mobile electronics [1], renewable energy deployment [2], and electric vehicles (EV) [2–4]. Conventional Li-ion batteries can benefit from an increase in reversible capacity, cycle life, and charge–discharge rates which come from modification of cell design and selection of novel active materials [2]. The cathode (positive electrode) has been shown to represent a critical component on the path towards realizing significantly improved Li-ion batteries [5–8]. Improvements in performance on the anode (e.g., material stability and long-term cycling) have pushed the envelope in Li-ion battery development [9–12]. However, the cathode determines the voltage potential in the battery and capacity limitations with the cathode have retarded further progress. State-of-the-art (SOA) cathode chemistries, including $LiNiCoAlO_2$ and Li-rich metal oxides have been shown to be excellent for energy-intensive applications. However, the impending battery needs will require new active materials and battery designs that are capable of high capacity at high voltages.

Transition metal oxide cathodes have displayed poor safety metrics due to thermal runaway associated with decomposition of the active material upon excessive delithiation (charging). This leads to release of oxygen, which reacts with internal battery materials, specifically

the electrolyte [13]. To improve the safety of Li-ion batteries, alternatives to $LiMO_2$ cathodes are being investigated, including the polyanion class of transition metal phosphates $LiMPO_4$ (M = Fe, Mn, Co, and Ni) [14]. $LiCoPO_4$, in particular, is of high interest due to its capability to achieve higher potentials versus $LiMO_2$ leading to higher energy densities up to 800 Wh kg^{-1} (based on the theoretical capacity and potential). Additionally, the thermal stability of $LiCoPO_4$ makes it a promising candidate for high energy applications [15].

Synthesis techniques for generating $LiMPO_4$ cathode include solid-state, hydrothermal, and solvothermal approaches. Solid-state synthesis has been the dominant technique to produce $LiMPO_4$ [5, 7, 8, 14–18]. Commercial $LiFePO_4$ is produced in this manner, which has shown good reproducibility and quality in electrochemical performance with a maximum capacity of 160 mAh g^{-1} [15]. Hydrothermal and sol–gel synthesis techniques have also been utilized to produce $LiMPO_4$, including $LiCoPO_4$, with capacities on the order of 60–70 mAh g^{-1} [19–22]. Solvothermal synthesis has been shown to achieve nanometer-sized particles and has been used to produce each of the phosphate analogs. Traditionally, solvothermal synthesis takes place at atmospheric conditions and at temperatures reaching 700 °C. The major disadvantage of using this particular synthesis technique is the long times (on the order of hours to days) needed to produce the desired product. An alternative to the traditional solvothermal approach utilizes microwaves. Microwave synthesis takes advantage of high energy radiation of a solution to reduce processing times to minutes. The microwave technique has been used to produce nanometer-sized $LiFePO_4$, $LiMnPO_4$, $LiCoPO_4$, and $LiNiPO_4$ with synthesis times ranging from 5 to 15 min and excellent reproducibility [23]. Intrinsic capacities for microwave-synthesized $LiCoPO_4$ have averaged 120 mAh g^{-1} [23]. Thus, utilization of microwave synthesis serves as an excellent opportunity to improve processing times and yield cathode materials with capacities that meet or exceed materials produced from other prominent synthesis techniques.

In this article, a systematic study of the synthesis of $LiCoPO_4$ cathode active material for Li-ion batteries is completed to understand the optimal conditions by which the electrochemical performance of this active material could be improved over recent reports. Microwave synthesis is utilized to produce the lithium cobalt phosphate with a specific focus on variations in molar ratios between base and acid content as it pertains to the performance of the material in a battery. Scanning electron microscopy (SEM), X-ray diffraction (XRD), and surface area are used to characterize the as-synthesized material. Electrochemical testing using a constant current–constant voltage (CC–CV) procedure is examined to determine conditions necessary for achieving maximum performance. An assessment of the optimal microwave synthesis conditions for yielding the highest capacity is presented and will be discussed.

2 Experimental

2.1 Synthesis of $LiCoPO_4$

$LiCoPO_4$ was synthesized via microwave synthesis following the procedure previously described [23]. Lithium hydroxide (LiOH, 98 % Sigma Aldrich) and cobalt(II) acetate tetrahydrate [$Co(CH_3COO)_2{\cdot}4H_2O$, Sigma Aldrich] were dissolved in tetraethylene glycol (TEG, Sigma Aldrich) using a Thinky ARE-310 planetary centrifugal mixer (Thinky Corporation, Japan) for 30 min at 2,000 rpm. To the mixture, 85 % phosphoric acid solution (H_3PO_4, Acros Organics) was added. The stoichiometric ratio between Li/Co/P was fixed at 1:1:1. Ammonium hydroxide (NH_4OH, Acros Organics) was added to maintain a ratio with H_3PO_4 (moles NH_4OH/moles H_3PO_4) between 0 and 1.5. The precursor solution (violet) was transferred to quartz vessels, sealed on a rotor, and loaded in a Synthos 3000 Microwave Synthesis Reactor (Anton Paar, USA). Solutions were irradiated for 15 min at 2.45 GHz and 1,200 W. The resultant pink precipitate was washed with acetone to remove all organic material and dried under vacuum at 200 °C for 2 h.

2.2 Characterization of as-synthesized material

As-synthesized $LiCoPO_4$ powders were characterized using SEM, XRD, and surface area analysis. SEM images were taken using a field-emission SEM (Hitachi, Japan) at an accelerating voltage of 2.0 kV at 15,000× magnification. XRD measurements were taken on a D2 Phaser benchtop XRD system (Bruker AXS, Germany) using Co Kα radiation ($\lambda = 1.789$ Å) scanning between 2θ of 10° and 80°. All samples were prepared by uniform packing of material in sample holders. Surface area measurements were performed using a NOVA 1000e high speed surface area and pore size analyzer (Quantachrome Instruments, USA). Samples were degassed for 24 h before nitrogen sorption experiments were started. The Brunauer–Emmett–Teller method was used to compute the surface area.

2.3 Electrochemical testing

$LiCoPO_4$ powders were combined with polyvinylidene fluoride (PVDF, Kynar) binder and Super C65 conductive carbon (Timcal) in a mass ratio of 80:10:10 $LiCoPO_4$/PVDF/Super C65. All solids were mixed in 1-methyl-2-pyrrolidinone (NMP) using a Thinky planetary centrifugal mixer until a uniform slurry was formed. The slurry was

cast on an aluminum current collector using a K Controller adjustable blade coater at a height of 300 μm and allowed to dry at 80 °C to evaporate the NMP. Post-drying thicknesses were 80–100 μm and all composites were calendered to reduce the composite thickness to 40–60 μm. Coin cells of the $LiCoPO_4$ electrodes were prepared using CR2032 coin cells. Li metal was used as the anode and Celgard 2325 served as the separator. Coin cell assembly was performed in an Ar-filled glove box. The electrolyte was composed of 1 M lithium hexafluorophosphate ($LiPF_6$) dissolved in ethylene carbonate (EC) and ethyl methyl carbonate (EMC) in a ratio of 1:2 by volume, respectively. Coin cells were cycled at 27 °C using an Arbin BT2000 32-channel battery cycler charging/discharging galvnostatically between 3 and 5 V at a specific current of 12 mA g^{-1} and holding with a CV step at 5 V to varying percentages of the initial CC before discharge.

3 Results and discussion

3.1 Characterization of $LiCoPO_4$

Characterization of the as-synthesized $LiCoPO_4$ included XRD, SEM, and surface area analysis using the BET method. Figure 1 shows the XRD patterns for the base-to-acid ratio conditions studied in this study. In all cases, there is excellent agreement between the experimental spectra and powder diffraction file (PDF) reference for $LiCoPO_4$ (ICDD# 01-085-0002). SEM images for each of the base-to-acid ratio samples are presented in Fig. 2. The images show distinct shapes including nanocubes and nanothumbs similar to previously reported studies [23]. The size of the nanoparticles ranging from 200 nm to over 1 μm. Variation in the particle size is attributed to the fact that microwave synthesis is limited in the parameters that can be used to control size (i.e., temperature and time); however, this approach is more favorable for achieving nanosized materials as compared to solid-state and hydrothermal syntheses [19]. Surface area of the active material is on average 4.6 ± 1.0 m^2 g^{-1} for all synthesis conditions.

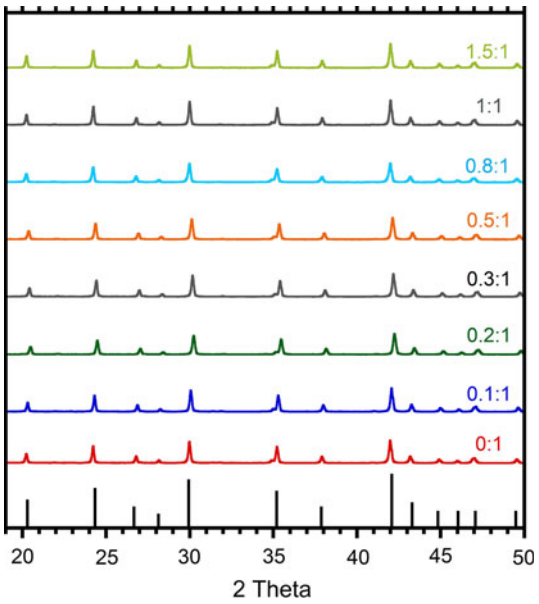

Fig. 1 XRD patterns for $LiCoPO_4$ prepared at base-to-acid ratios of 0, 0.1, 0.2, 0.3, 0.5, 0.8, 1, and 1.5 taken on a Bruker D2 PHASER XRD system using Co Kα radiation. PDF reference for $LiCoPO_4$ represented by *black sticks* (ICDD# 01-085-0002)

3.2 Base-to-acid ratio impacts on electrochemical capacity

The focus of this study is to determine an optimal condition for achieving a high capacity cathode active material via microwave synthesis. Previous studies indicate that the synthesis of $LiCoPO_4$ requires the addition of a source of OH^- to achieve basic conditions [19, 23], but the degree by which NH_4OH is needed to produce $LiCoPO_4$ with optimal performance has not been reported. In this study, the amount of NH_4OH addition is varied based on a molar ratio between the base and acid (H_3PO_4) from 0 to 1.5. $LiCoPO_4$ production is achievable at all base-to-acid ratios tested, including the case where no NH_4OH is added to the solution. Electrochemical analysis was performed using coin cells to understand the capabilities of the as-synthesized materials. The cathode (active material, PVDF, and conductive carbon) was placed opposite lithium foil and tested between 3 and 5 V versus Li/Li^+. Figure 3a shows the discharge capacities for the series of base-to-acid ratios examined during this study. The highest intrinsic capacity observed is for a base-to-acid ratio of 0.2:1 with a maximum capacity of 128 mAh g^{-1}. This capacity is higher than the average capacity of 120 mAh g^{-1} which has been reported by others [21, 23–25]. Figure 3b summarizes the discharge capacities as a function of the base-to-acid ratios to illustrate the effects NH_4OH has on the discharge capacity of the cathode active material. The capacity is seen to significantly decrease as the base-to-acid ratio increases with the lowest capacity of 59 mAh g^{-1} at 1.5:1 base-to-acid ratio. This decrease in capacity at the higher base-to-acid ratios is likely attributed to alterations in the pH of the solution which affects the resulting product after reaction. Previous report for hydrothermal synthesis of $LiCoPO_4$ showed that the pH of the solution significantly impacted the size and morphology of the final product after reaction [19]. A microwave-assisted hydrothermal synthesis of $LiCoPO_4$ [26], following the procedure of [19], maintained the pH of the $LiCoPO_4$ solution at 9.9 to avoid the production of cobalt phosphate

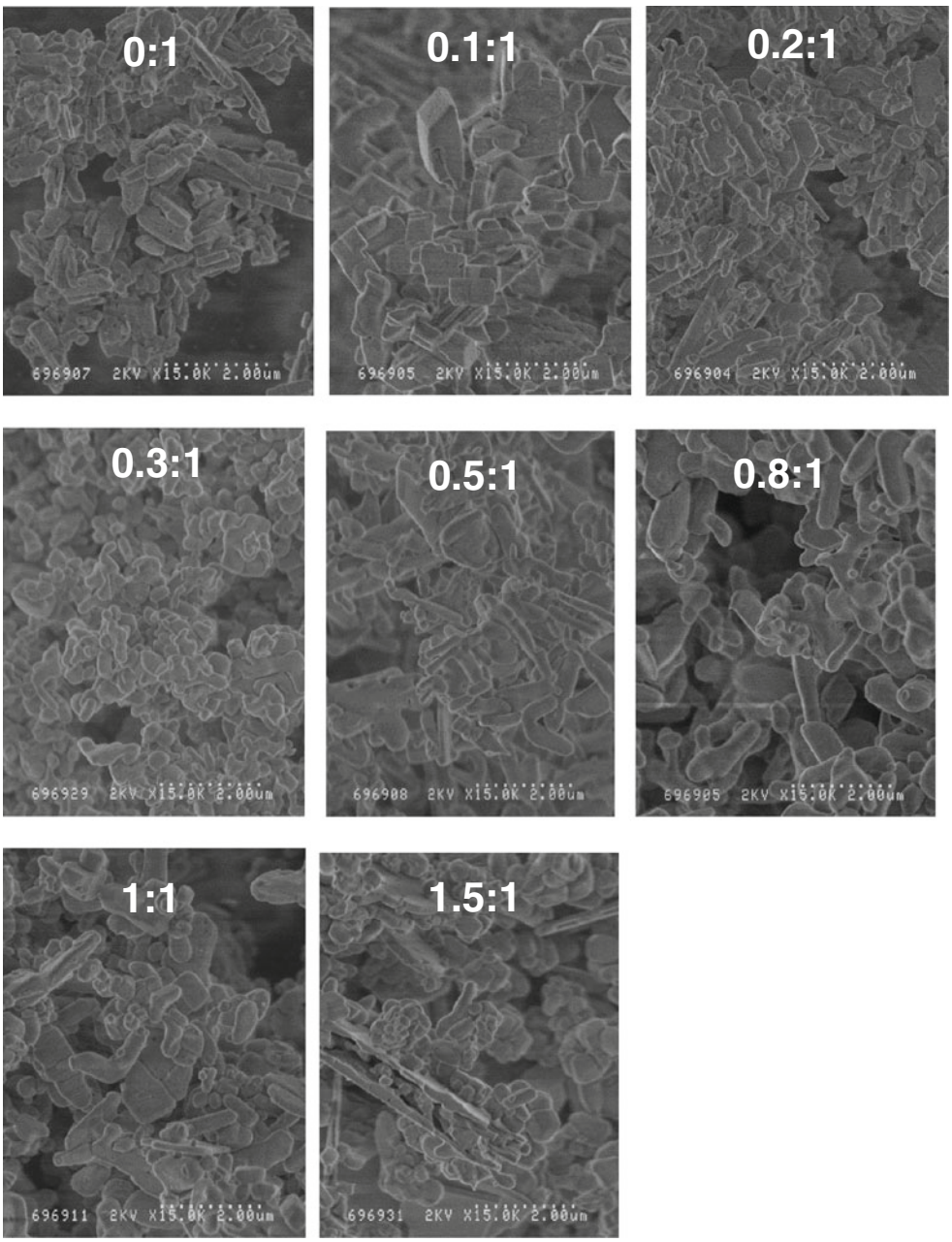

Fig. 2 SEM images of $LiCoPO_4$ representing powders synthesized at 0:1, 0.1:1, 0.2:1, 0.3:1, 0.5:1, 0.8:1, 1:1, and 1.5:1 base-to-acid ratios. All SEM scans taken at ×15,000 magnification

hydrate, which forms under acidic conditions. The researchers demonstrated cubes of the material with particles sizes >1 μm yielded capacities of only 50 mAh g^{-1} attributing the result to the conditions of the reactant solution. Therefore, the pH can lead to changes in the physical and electronic properties of the active material which in turn affects the electrochemical performance as has been shown through this analysis. In this study, the pH of the 0.2:1 case was measured to be ~8.5. All subsequent experimental results are reported based on $LiCoPO_4$ synthesized at a base-to-acid ratio of 0.2:1.

3.3 Charging protocol effects on capacity

Previous work with $LiFePO_4$ and $LiMnPO_4$ has shown that incorporation of a CV step promotes an increase in discharge capacity due to achieving a fully delithiated state after charging [27, 28]. An analysis was done to understand the effects of including a CV step during charging of the $LiCoPO_4$ cathode. Four CV conditions were considered: No CV step, CV @ 5 V versus Li/Li^+ to 5 % of the initial CC (5 % CC), CV to 25 % CC, and CV to 50 % CC. Coin cells were

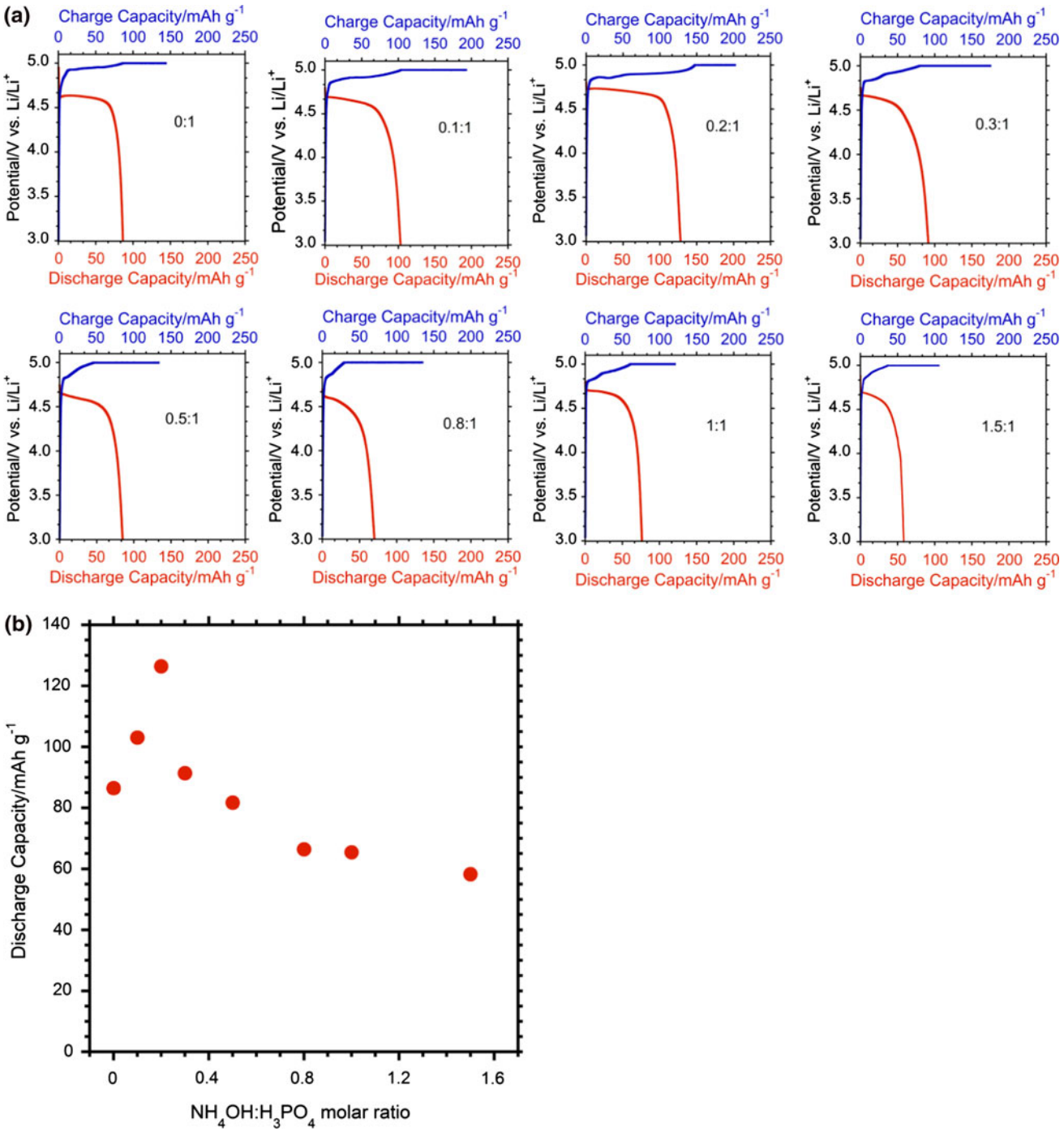

Fig. 3 **a**, **b** Charge–discharge capacity comparison for $LiCoPO_4$ synthesized at NH_4OH:H_3PO_4 ratios between 0 and 1.5. Half cells cycled between 3 and 5 V with a CV step to 5 % CC. All cells discharged at an effective current rate of 0.1*C*

charged and discharged between 3 and 5 V. Figure 4a shows the discharge profiles for each of the cases tested. Not including a CV step yields the lowest capacity of 91 mAh g^{-1} most likely due to an incomplete delithiation of $LiCoPO_4$. It is known that $LiCoPO_4$ undergoes a phase change to $CoPO_4$ as the cathode is charged [16]. As the CV step is extended from 50 % CC to 5 % CC, thereby increasing the time at which the cells are in the charge phase, the discharge capacity improves significantly up to 128 mAh g^{-1} for a CV step to 5 % CC. This indicates that a fully delithiated state is potentially reached therefore maximizing lithiation on discharge as suggested by previous studies [27, 28]. It is noted that the first cycle coulombic efficiency for all cases is ~60 %. Figure 4b shows the cycling behavior for each of the CV cases. In all

four conditions, there is a decrease in the capacity over the course of 10 cycles with a 20 % capacity fade for the best case of a CV to 5 % CC. The 80 % capacity retention after 10 cycles for the intrinsic material is significantly better than recent reports combining $LiCoPO_4$ with a conductive source like carbon nanotubes where 60 % capacity retention was observed after 10 cycles [29]. It is known that the organic electrolyte will break down above a voltage of 4.6 V [14, 23]. Given that $LiCoPO_4$ requires a minimum potential of 4.8 V for charge and discharge, the loss in capacity can most likely be associated with this phenomenon. Improvements in the electrolyte will be necessary in order to overcome this barrier and achieve a stable capacity necessary for applications of interest. However, progress with $LiCoPO_4$ continues towards development of a stable active material that can be used in advanced battery applications.

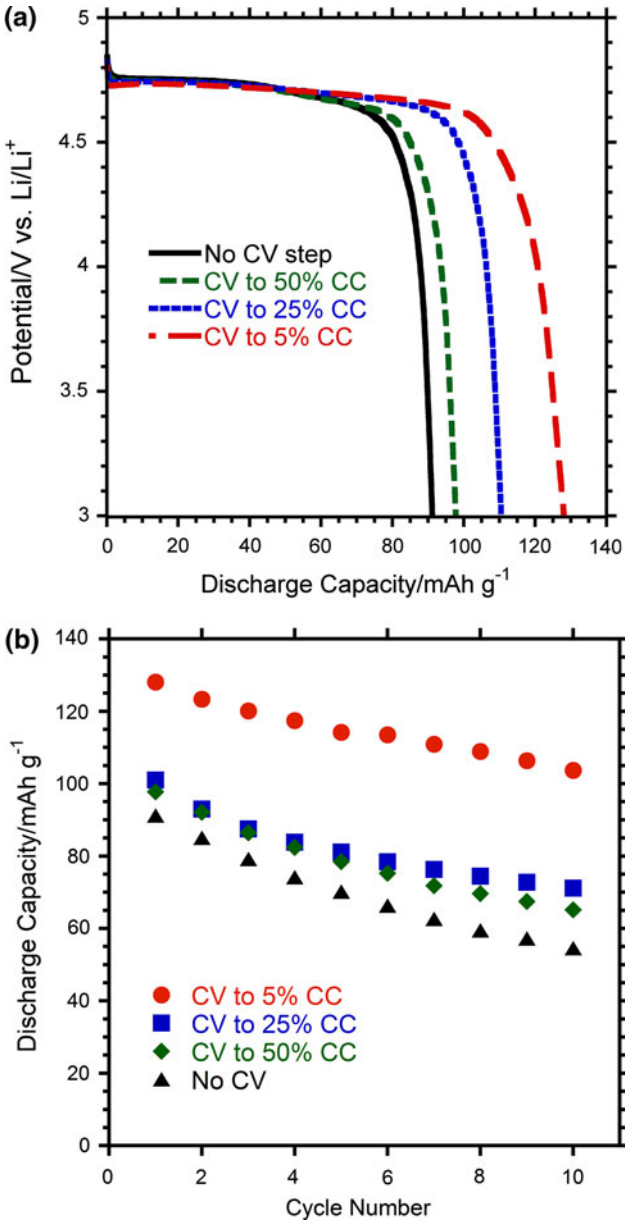

Fig. 4 **a** Discharge capacities of $LiCoPO_4$ (0.2:1 base-to-acid) as a function of charging protocol. Half cells charged to 5 V and held with (i) no CV and under CV (5 V) conditions to (ii) 50 %, (iii) 25 %, and (iv) 5 % the initial CC. Electrolyte used was 1 M $LiPF_6$ 1:2 EC:EMC (v/v). **b** Cycling profile for each CV condition up to 10 cycles

3.4 Rate comparison for $LiCoPO_4$

The as-synthesized $LiCoPO_4$ active material was further analyzed for its capacity performance under different rate conditions. The active material synthesized under a 0.2:1 base-to-acid condition was cycled at an effective C-rate of 0.1*C*, 0.2*C*, 0.5*C*, 1*C*, and 2*C*, based on the measured capacity in Fig. 3a, with a CV step to 5 % of the initial CC value. Figure 5 presents the results of this analysis. The capacity is observed to remain above 100 mAh g^{-1} for both 0.1*C* and 0.2*C* with a voltage plateau around 4.7 V versus Li/Li^+. At 0.5*C* and above, the capacity is below 100 mAh g^{-1} and the voltage plateau decreases. However, the rate performance of the as-synthesized material in this study is improved over previously published results using a lower content of conductive carbon (10 vs. 12.5 wt%), which suggests that the semi-optimized synthesis conditions leads to higher performing active material.

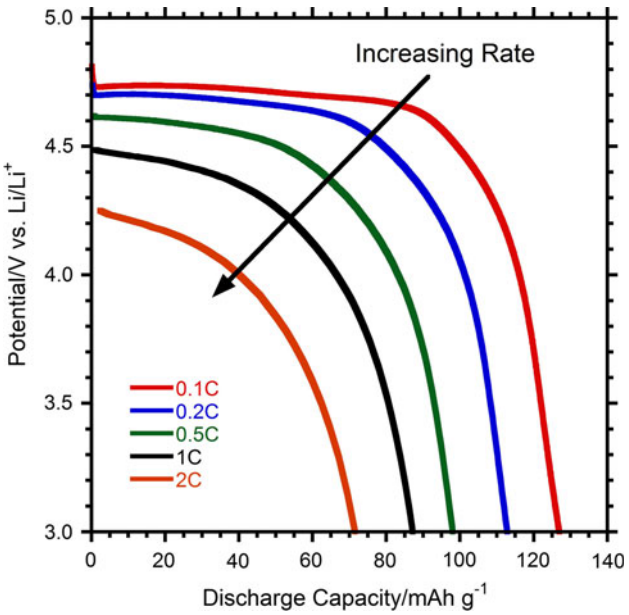

Fig. 5 Capacity comparison for intrinsic $LiCoPO_4$ for rates between 0.1*C* and 2*C*. Half cells cycled between 3 and 5 V with a CV step to 5 % CC

3.5 Comparison against alternative synthesis approaches

Synthesis of $LiCoPO_4$, as well as other lithium transition metal phosphates, has been ongoing for more than a decade. As new synthesis techniques evolve, improvement in performance of the lithium transition metal phosphates has been realized. Figure 6 shows the progression in the capacity of $LiCoPO_4$ from 2000 to present. Solid-state synthesis, which is the standard method for synthesizing $LiCoPO_4$ on the bulk scale, has seen a capacity increase from 100 mAh g^{-1} in 2001 to 120 mAh g^{-1} in 2004. Limited work has been done with hydrothermal synthesis with a maximum capacity of 63 mAh g^{-1} reported. Recent synthesis approaches, such as microwave synthesis, have reported capacity increases for $LiCoPO_4$ from 93 to 128 mAh g^{-1} based upon this study. It is noted that the values reported in Fig. 6 are the intrinsic capacities of $LiCoPO_4$ that has not been treated with a carbon source to improve the capacity. It is important to note that this summary is meant to illustrate the highest values reported in the literature realizing that the charging protocol (i.e., charge rate, cutoff voltage, CV step, etc.) will influence the results. As refinement of current synthesis techniques and introduction of novel approaches continues, it is expected that the intrinsic capacities reported will continue to increase. Additionally, the safety advantage of lithium transition metal phosphates continues the motivation for studying $LiCoPO_4$ for high voltage and high energy density applications. Thermal stability studies on these polyanion class of cathodes shows less likelihood of O_2 evolution from the delithiated state therefore reducing thermal runaway [30–33]. As such, there is a strategic advantage to using $LiCoPO_4$ for high voltage applications when compared to current-market cathode active materials [e.g., lithium nickel cobalt aluminum oxide (NCA)]. Above all, a high voltage electrolyte must be addressed for significant progress to be made. Once a suitable electrolyte for high voltage cathodes is realized, it is anticipated materials like $LiCoPO_4$ will be sustainable in future Li-ion applications.

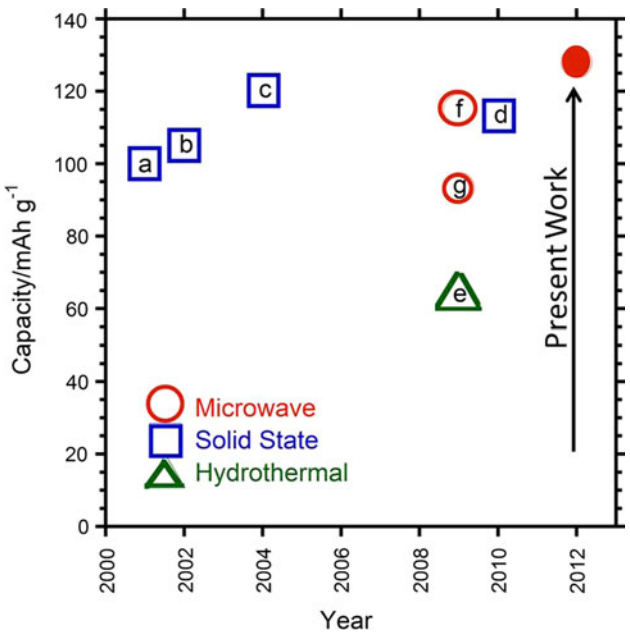

Fig. 6 Capacity comparison for cycle 1 of intrinsic $LiCoPO_4$ (not modified or carbon treated) synthesized via microwave, solid-state, and hydrothermal methods between 2000 and 2012. *Solid red circle* represents capacity value reported in this study (128 mAh g^{-1}). Values taken from following references (*a*) [15], (*b*) [7], (*c*) [5], (*d*) [34], (*e*) [19], (*f*) [23], (*g*) [25]

4 Conclusion

A systematic analysis of the synthesis and characterization of $LiCoPO_4$ via a microwave synthesis technique has been presented. Synthesis of $LiCoPO_4$ at various base-to-acid ratios shows an optimal ratio of 0.2:1 for achieving the highest reported intrinsic capacity of 128 mAh g^{-1}. Variation of the base content during synthesis, corresponding to a change in pH, is shown to affect the end product, leading to significant differences in the discharge capacity. A CV protocol at 5 V versus Li/Li^+ to 5 % of the initial CC (5 % CC) represents the best case scenario for achieving the maximum attainable capacity. Cycling of the intrinsic $LiCoPO_4$ material shows 80 % capacity retention after 10 cycles, representing an improvement over carbon-treated $LiCoPO_4$. Fade in the capacity is attributed to electrolyte degradation which is a prominent issue with the advancement of high voltage cathodes. An assessment of different synthesis techniques to produce $LiCoPO_4$ shows that microwave syntheses yield the highest intrinsic capacity results to date for this cathode active material. With continued refinement in electrolyte chemistry and the enhanced safety attributes, it is anticipated $LiCoPO_4$ will be a viable option for future Li-ion battery applications.

Acknowledgments We acknowledge funding support from the Department of Energy (DE-FG36-08 GO88110) and RIT Office for Diversity & Inclusion. We also acknowledge financial support from the U.S. Government including a Grant from the Intelligence Community Postdoctoral Research Fellowship Program through funding from the Office of the Director of National Intelligence. R.A.D. acknowledges graduate student funding from a GAANN fellowship through the RIT Microsystems Engineering Ph.D. Program.

References

1. Endo M, Kim C, Nishimura K, Fujino T, Miyashita K (2000) Recent development of carbon materials for Li ion batteries. Carbon 38:183–197
2. Daniel C (2008) Materials and processing for lithium-ion batteries. JOM J Miner Met Mater Soc 60(9):43–48

3. Howell D (2009) Progress Report for Energy Storage Research and Development. U.S. Department of Energy, Washington, DC
4. Goodenough JB, Kim Y (2010) Challenges for rechargeable Li batteries. Chem Mater 22(3):587–603. doi:10.1021/cm901452z
5. Wakihara M, Nakayama M, Goto S, Uchimoto Y, Kitajima Y (2004) Changes in electronic structure between cobalt and oxide ions of lithium cobalt phosphate as 4.8-V positive electrode material. Chem Mater 16(18):3399–3401. doi:10.1021/cm049230t
6. Shih HC, Chen YC, Chen JM, Hsu CH, Lee JJ, Lin TC, Yeh JW (2010) Electrochemical and structural studies of LiCo(1/3)Mn(1/3)Fe (1/3)PO(4) as a cathode material for lithium ion batteries. J Power Sources 195(19):6867–6872. doi:10.1016/j.jpowsour.2010.01.058
7. Lloris JM, Vicente CP, Tirado JL (2002) Improvement of the electrochemical performance of LiCoPO(4) 5 V material using a novel synthesis procedure. Electrochem Solid State Lett 5(10): A234–A237. doi:10.1149/1.1507941
8. Padhi AK, Nanjundaswamy KS, Goodenough JB (1997) Phospho-olivines as positive-electrode materials for rechargeable lithium batteries. J Electrochem Soc 144(4):1188–1194
9. Dileo RA, Castiglia A, Ganter MJ, Rogers RE, Cress CD, Raffaelle RP, Landi BJ (2010) Enhanced capacity and rate capability of carbon nanotube based anodes with titanium contacts for lithium ion batteries. ACS Nano 4(10):6121–6131. doi: 10.1021/nn1018494
10. DiLeo RA, Frisco S, Ganter MJ, Rogers RE, Raffaelle RP, Landi BJ (2011) Hybrid germanium nanoparticle-single-wall carbon nanotube free-standing anodes for lithium ion batteries. J Phys Chem C 115(45):22609–22614. doi:10.1021/jp205992w
11. DiLeo RA, Ganter MJ, Raffaelle RP, Landi BJ (2010) Germanium-single-wall carbon nanotube anodes for lithium ion batteries. J Mater Res 25(8):1441–1446. doi:10.1557/jmr.2010.0184
12. Landi BJ, Ganter MJ, Cress CD, DiLeo RA, Raffaelle RP (2009) Carbon nanotubes for lithium ion batteries. Energy Environ Sci 2(6):638–654. doi:10.1039/b904116h
13. Ganter MJ, DiLeo RA, Schauerman CM, Rogers RE, Rafaelle RP, Landi BJ (2011) Differential scanning calorimetry analysis of an enhanced $LiNi_{0.8}Co_{0.2}O_2$ cathode with single wall carbon nanotube conductive additives. Electrochim Acta 56:7272–7277
14. Bramnik NN, Nikolowski K, Trots DM, Ehrenberg H (2008) Thermal stability of $LiCoPO_4$ cathodes. Electrochem Solid State Lett 11(6):A89–A93. doi:10.1149/1.2894902
15. Okada S, Sawa S, Egashira M, Yamaki J, Tabuchi M, Kageyama H, Konishi T, Yoshino A (2001) Cathode properties of phospho-olivine $LiMPO_4$ for lithium secondary batteries. J Power Sources 97–8:430–432
16. Bramnik NN, Nikolowski K, Baehtz C, Bramnik KG, Ehrenberg H (2007) Phase transitions occurring upon lithium insertion-extraction of $LiCoPO_4$. Chem Mater 19(4):908–915. doi:10.1021/cm062246u
17. Koleva V, Zhecheva E, Stoyanova R (2010) Ordered olivine-type lithium–cobalt and lithium–nickel phosphates prepared by a new precursor method. Eur J Inorg Chem 26:4091–4099. doi:10.1002/ejic.201000400
18. Okada S, Ueno M, Uebou Y, Yamaki J (2005) Fluoride phosphate Li(2)COPO(4)F as a high-voltage cathode in Li-ion batteries. J Power Sources 146(1–2):565–569. doi:10.1016/j.jpowsour.2005.03.149
19. Ma JF, Huang XA, Wu PW, Hu YM, Dai JH, Zhu ZB, Chen HY, Wang HF (2005) Hydrothermal synthesis of $LiCoPO_4$ cathode materials for rechargeable lithium ion batteries. Mater Lett 59(5):578–582. doi:10.1016/j.matlet.2004.10.049
20. Xia DG, Zhao YJ, Wang SJ, Zhao CS (2009) Synthesis and electrochemical performance of LiCoPO(4) micron-rods by dispersant-aided hydrothermal method for lithium ion batteries. Rare Met 28(2):117–121. doi:10.1007/s12598-009-0023-5
21. Poovizhi PN, Selladurai S (2011) Study of pristine and carbon-coated LiCoPO(4) olivine material synthesized by modified sol–gel method. Ionics 17(1):13–19. doi:10.1007/s11581-010-0496-0
22. Yang JS, Xu JJ (2006) Synthesis and characterization of carbon-coated lithium transition metal phosphates $LiMPO_4$ (M = Fe, Mn, Co, Ni) prepared via a nonaqueous sol–gel route. J Electrochem Soc 153(4):A716–A723. doi:10.1149/1.2168410
23. Manthiram A, Murugan AV, Muraliganth T, Ferreira PJ (2009) Dimensionally modulated, single-crystalline LiMPO(4) (M = Mn, Fe, Co, and Ni) with nano-thumblike shapes for high-power energy storage. Inorg Chem 48(3):946–952. doi:10.1021/ic8015723
24. Badsar M, Edrissi M (2010) Synthesis and characterization of different nanostructures of cobalt phosphate. Mater Res Bull 45(9):1080–1084. doi:10.1016/j.materresbull.2010.06.022
25. Li HH, Jin J, Wei JP, Zhou Z, Yan J (2009) Fast synthesis of core–shell $LiCoPO_4$/C nanocomposite via microwave heating and its electrochemical Li intercalation performances. Electrochem Commun 11(1):95–98. doi:10.1016/j.elecom.2008.10.025
26. Murugan AV, Muraliganth T, Manthiram A (2009) One-pot microwave-hydrothermal synthesis and characterization of carbon-coated $LiMPO_4$ (M = Mn, Fe, and Co) cathodes. J Electrochem Soc 156(2):A79–A83. doi:10.1149/1.3028304
27. Liao LX, Zuo PJ, Ma YL, Chen XQ, An YX, Gao YZ, Yin GP (2012) Effects of temperature on charge/discharge behaviors of $LiFePO_4$ cathode for Li-ion batteries. Electrochim Acta 60: 269–273. doi:10.1016/j.electacta.2011.11.041
28. Doan TNL, Taniguchi I (2011) Cathode performance of LiMnPO(4)/C nanocomposites prepared by a combination of spray pyrolysis and wet ball-milling followed by heat treatment. J Power Sources 196(3):1399–1408. doi:10.1016/j.jpowsour.2010.08.067
29. Dimesso L, Forster C, Jaegermann W, Khanderi JP, Tempel H, Popp A, Engstler J, Schneider JJ, Sarapulova A, Mikhailova D, Schmitt LA, Oswald S, Ehrenberg H (2012) Developments in nanostructured $LiMPO_4$ (M = Fe, Co, Ni, Mn) composites based on three dimensional carbon architecture. Chem Soc Rev 41(15): 5068–5080. doi:10.1039/c2cs15320c
30. Martha SK, Haik O, Zinigrad E, Exnar I, Drezen T, Miners JH, Aurbach D (2011) On the thermal stability of olivine cathode materials for lithium-ion batteries. J Electrochem Soc 158(10): A1115–A1122. doi:10.1149/1.3622849
31. Ben Mayza A, Ramanathan M, Radhakrishnan R, Ha S, Ramani V, Prakash J, Zaghib K (2011) Thermal characterization of $LiFePO_4$ cathode in lithium ion cells. ECS Trans 35(34): 177–183. doi:10.1149/1.3654216
32. Zhou MJ, Zhao LW, Okada S, Yamaki J (2011) Thermal characteristics of a FeF_3 cathode via conversion reaction in comparison with $LiFePO_4$. J Power Sources 196(19):8110–8115. doi: 10.1016/j.jpowsour.2011.05.042
33. Joachin H, Kaun TD, Zaghib K, Prakash J (2009) Electrochemical and thermal studies of carbon-coated $LiFePO_4$ cathode. J Electrochem Soc 156(6):A401–A406. doi:10.1149/1.3106121
34. Jang IC, Lim HH, Lee SB, Karthikeyan K, Aravindan V, Kang KS, Yoon WS, Cho WI, Lee YS (2010) Preparation of $LiCoPO_4$ and $LiFePO_4$ coated $LiCoPO_4$ materials with improved battery performance. J Alloy Compd 497(1–2):321–324. doi:10.1016/j.jallcom.2010.03.055